Electronic Supplementary Material (ESI) for Environmental Science: Nano.

Supporting Information

Nano-biochar modulates the formation of iron plaque through facilitating iron-involved redox reactions on aquatic plant root surfaces

Shiguo Gu [a], Fei Lian [b*], Yaru Han [a], Sarasadat Taherymoosavi [c], David Mitchell [d], Stephen Joseph [c,e], Zhenyu Wang [a*], and Baoshan Xing [f]

[a] Institute of Environmental Processes and Pollution Control, and School of Environment and Civil Engineering, Jiangnan University, Wuxi 214122, China

[b] School of Energy and Environmental Engineering, Hebei University of Technology, Tianjin 300401, China

[c] School of Materials Science and Engineering, University of NSW, Kensington, NSW 2052, Australia

[d] Electron Microscopy Centre, AIIM Building, Innovation Campus, University of Wollongong, North Wollongong, NSW 2517, Australia

[e] Institute for Superconducting and Electronic Materials and School of Physics, University of Wollongong, NSW 2522, Australia

[f] Stockbridge School of Agriculture, University of Massachusetts, Amherst, Massachusetts 01003, United States

*Corresponding authors:

Tel: +86 022-60435775; email: lianfei2000@126.com (Fei Lian);

Tel: +86 0510 85911123; email: wang0628@jiangnan.edu.cn (Zhenyu Wang)

Number of pages: 14

Number of Figures: 10

Number of Tables: 4

Text S1: The fractionation of nano-BC from bulk-BC suspension

The BC powders were mixed with DI water to obtain BC suspensions and then were set quiescently for 2 h to make the majority of bulk-BC deposit. The upper layer of suspension was pipetted out and then refilled with DI water. This extraction procedure was repeated several times until the upper layer of suspension had negligible Tyndall effect. All the pipetted suspensions were combined and centrifuged at 10, 000 rpm for 30 min. The supernatant after centrifugation was freeze-dried to obtain nano-BC.

Text S2: Electrochemical measurements of nano-BC

Glassy carbon electrode (diameter 3 mm), platinum spiral wire, and Ag/AgCl (3 mol/L KCl) were used as working, counter, and reference electrodes, respectively. The cylinder (9 mL) was added phosphate buffer (0.1 mol/L KCl, pH = 7) and equilibrated to a desired redox potential. Subsequently, 100 μL of stock solution (10 mmol/L) of the electron transfer mediators zwitterionic viologen 4,4'-bipyridinium-1,1'-bis(2-ethylsulfonate) (in MER) or 2,2'-azino-bis(3-ethylbenzothiazoline-6-sulfonic acid) diammonium salt (in MEO) were added to the cells, resulting in reductive and oxidative current peaks, respectively. After reattainment of constant background currents, 200 μL of the nano-BC suspension (10 mg/L) were pipetted into the cells. The resulting reductive and oxidative current peaks were integrated to yield the electron accepting capacities (EAC) and donating capacities (EDC) (mmol e^-/g) of the added nano-BCs. All the measurements were performed in triplicates.

Text S3: the plate-counting assays

Rice seedlings with the same growth were transferred into 500 mL suspension of nano-

BC in the artificial rhizosphere pore water and followed by the addition of $FeSO_4 \cdot 7H_2O$ (50 mg/L) stock solution to form IP along root surfaces and cultivated for 2 days. Bottles receiving only artificial rhizosphere pore water instead of BC suspension were used as control. After harvest, the rice roots were rinsed by DI water to remove root impurities, and then the microorganisms were collected by ultrasound (30 mins). Aliquots (0.1mL) of 10^3 or 10^4 dilutions of the washings from rice roots, prepared in sterile water, were evenly spread on Luria-Bertani medium (10 g/L NaCl, 10 g/L tryptone, and 5 g/L yeast extract). Each dilution scheme was executed in triplicate by completing three separate dilution experiments. After 72 h of incubation at 30°C, and plate counts were conducted on each dilution.

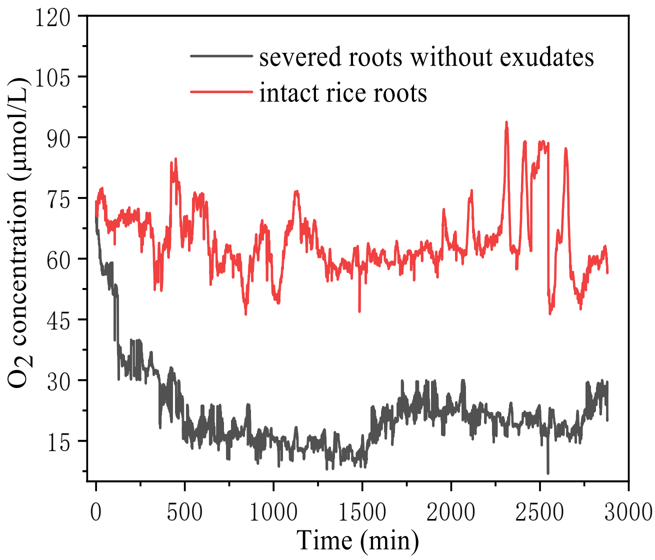

Fig. S1. Release of oxygen from the intact rice roots and severed roots without exudates. The data were indicative of the higher vitality of the intact rice roots.

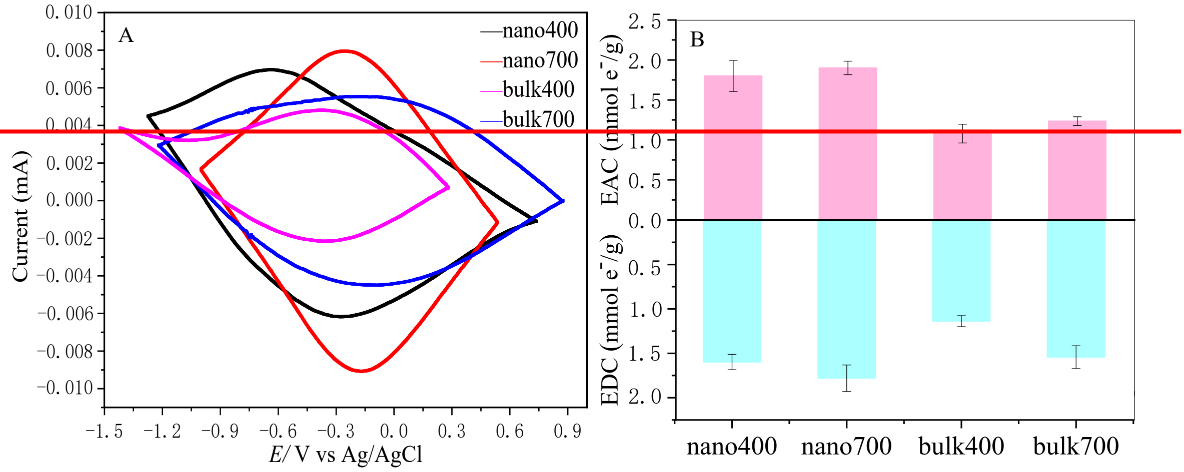

Fig. S2. Electrochemical characterization of bulk- and nano-BCs: (A) cyclic voltammetry of bulk-and nano-BCs prepared at 400 and 700 ^{o}C, respectively; and (B) electron accepting and donating capacity (EAC and EDC) of bulk- and nano-BCs on the basis of BC mass.

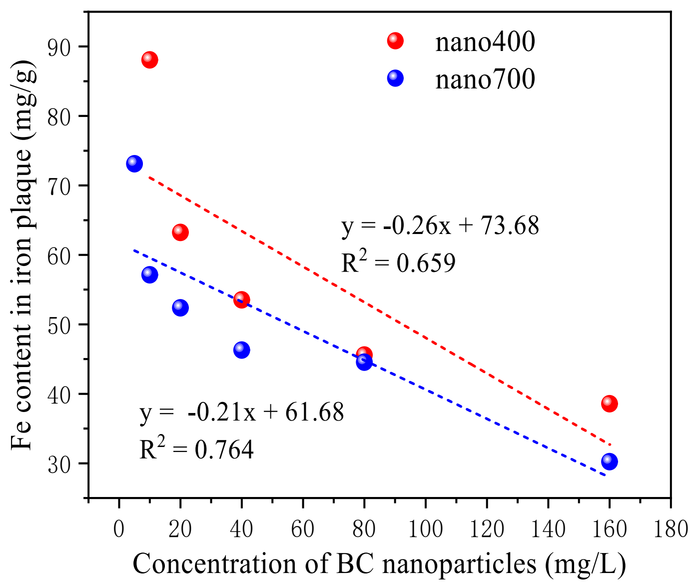

Fig. S3. The negative relationship between excess dosage of nano-BC and Fe content in iron plaque on rice roots.

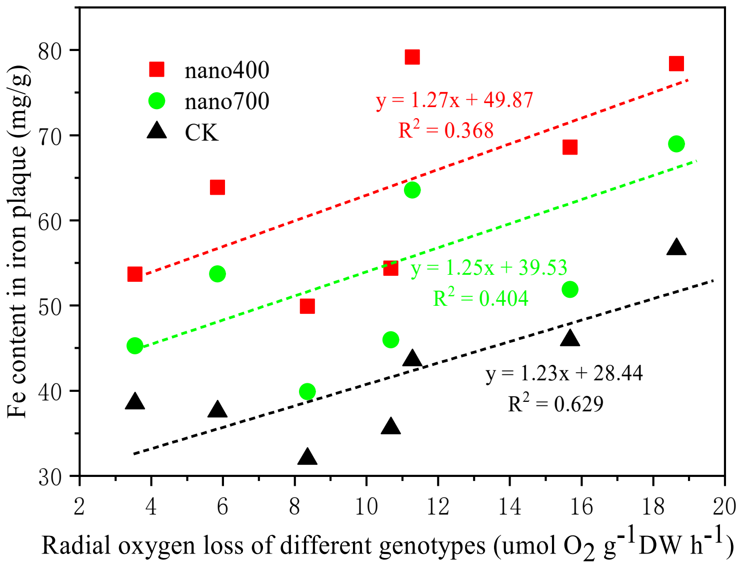

Fig. S4. Relationship between Fe content in plaque and the rate of radial oxygen loss of 7 rice genotypes in the presence and absence of nano-BCs, respectively. The concentration of Fe(II), nano400, and nano700 was 50 mg/L, 5.0 mg/L, and 2.5 mg/L, respectively. The tested rice genotypes included: 1#: Yueyou No.9113, Yueyang Institute of Agricultural Sciences, Hunan, China; 2#: Fupin Jiangsu academy of agricultural sciences, Nanjing, China; 3#: Zhongzao No.22, China National Rice Research Institute, Hangzhou, China; 4#: X24, Agro-Environmental protection Institute, Ministry of Agriculture; 5#: R705, Anhui Academy of Academy of Agricultural Sciences, Hefei, China; 6#: Nan Jing No.9108, Jiangsu academy of agricultural sciences, Nanjing, China; 7#: Hunan Hybrid rice research center, Changsha, China.

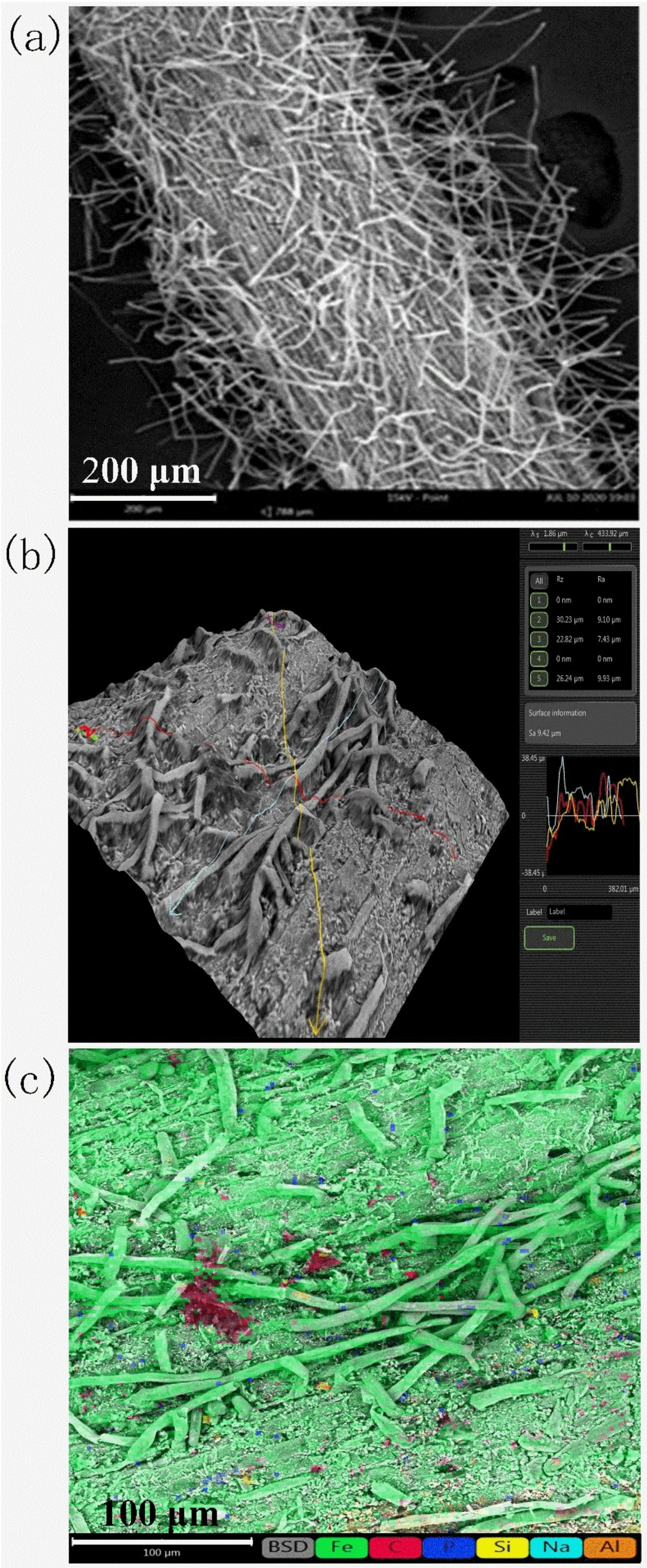

Fig. S5. SEM images and 3D topological mapping with EDS of plaque layer on control roots. (a) A low magnification backscattered SEM image showing plaque layer of the control roots surrounded by roots hairs and fungi; (b) 3D topological mapping with analysis of height variations of plaque layer; and (c) EDS showing the distribution of the main elements.

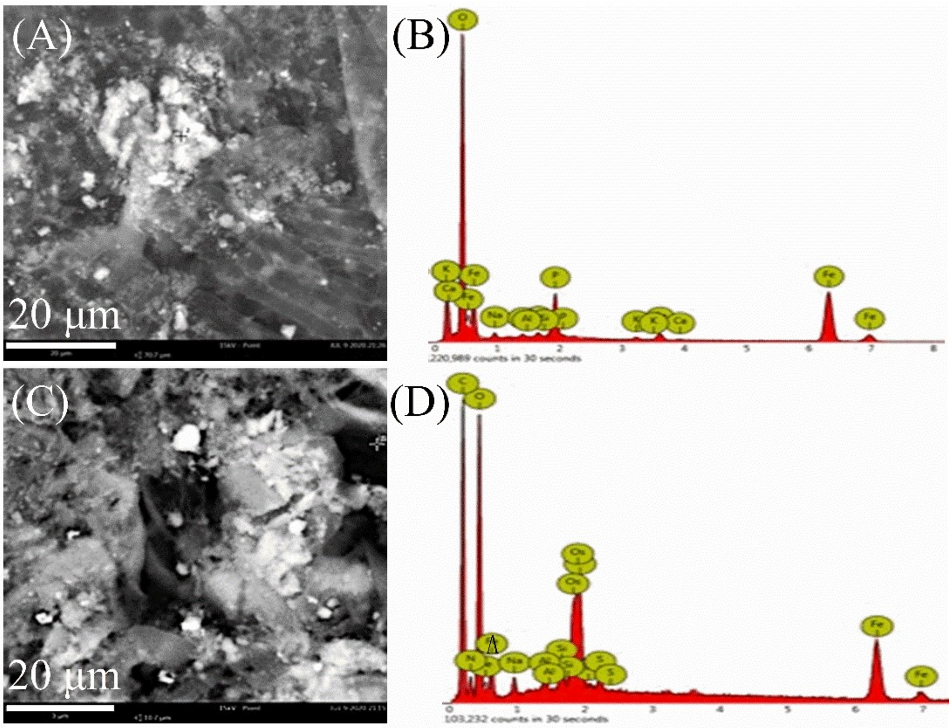

Fig. S6. A) Backscattered SEM image of biochar surface embedded in the plaque layer; B) EDS spectrum showing a significant concentration of different minerals on the surfaces; C) high magnification of the mineralized area in A with osmium and relative high concentration of N and S indicating micro-organisms growing in a biofilm.

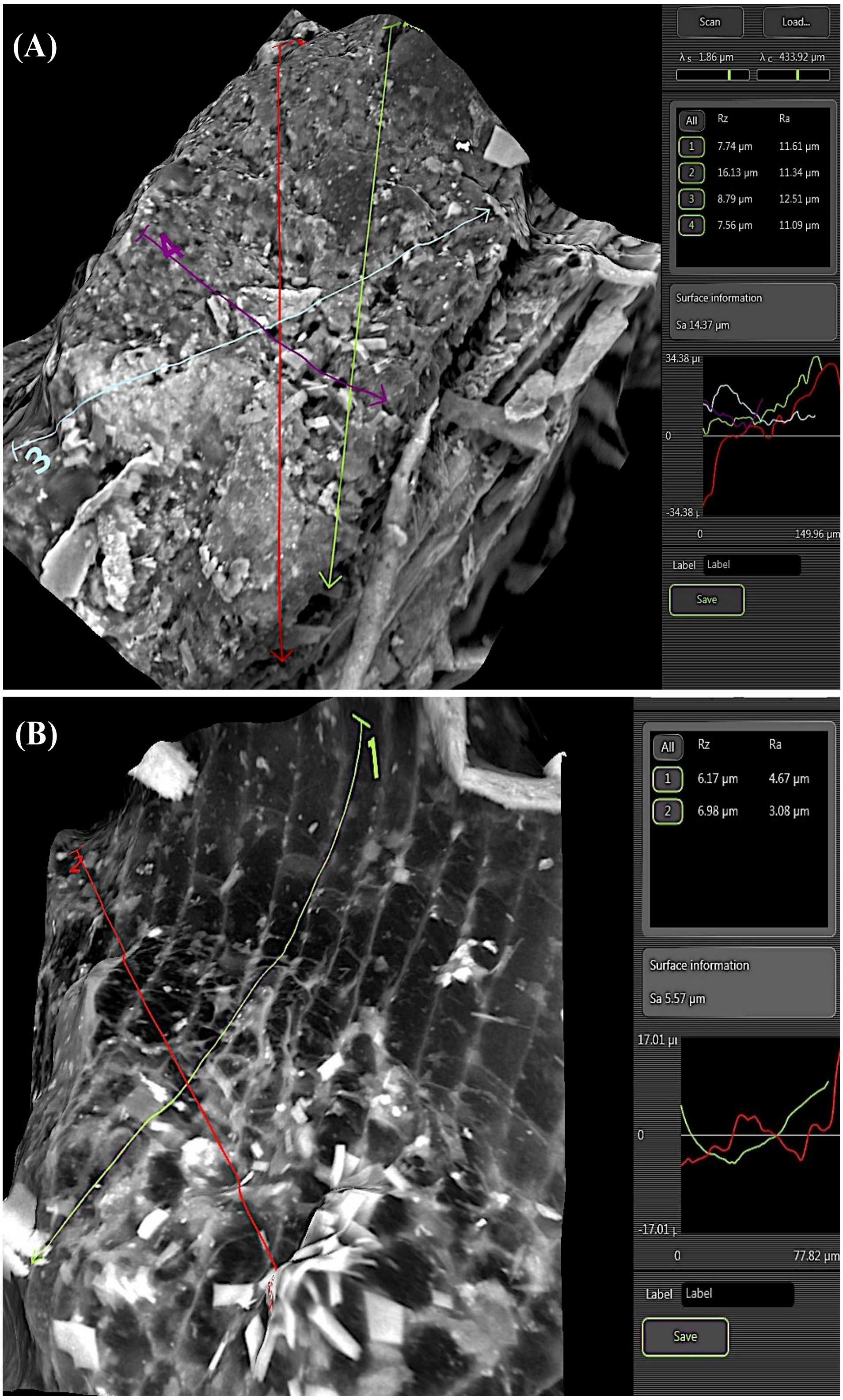

Fig. S7. 3D topographical maps of BC (nano400) surface embedded in the plaque layer (A and B) and high magnification of the BC area in the panel A (C and D).

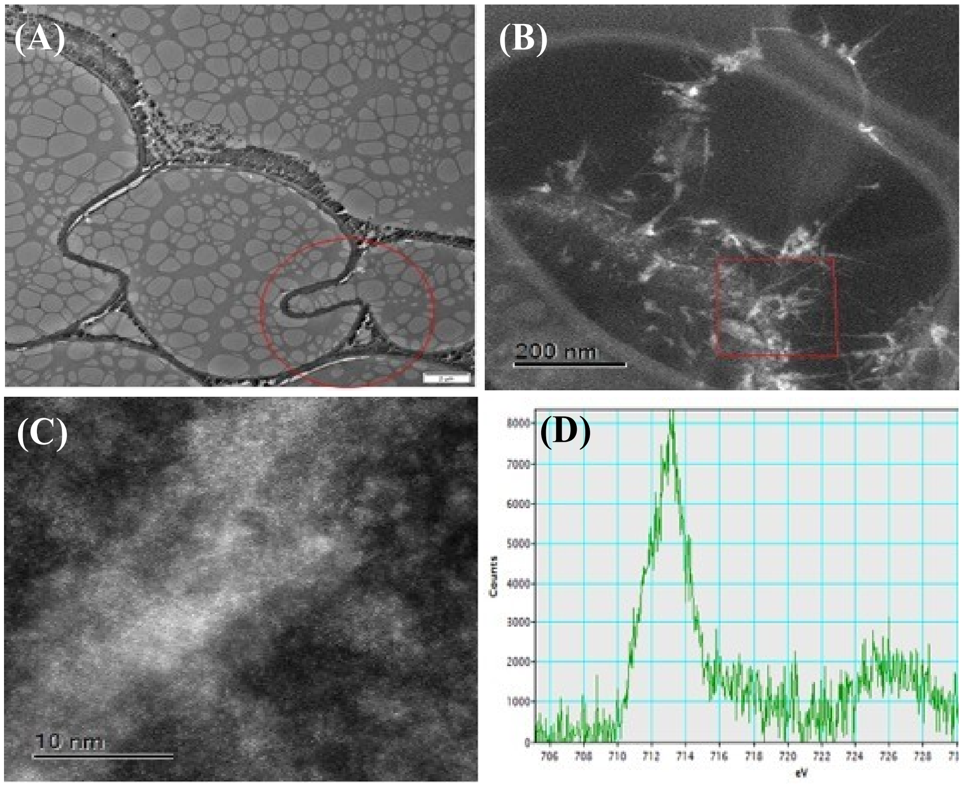

Fig. S8. (A) Bright field images of inside of control roots with an area consisting of iron nanoparticles (B and C) and EELS spectrum (D) indicating the nanoparticles could be magnetite or a mixture of other Fe^{2+} and Fe^{3+} compounds (possibly goethite or ferrihydrite).

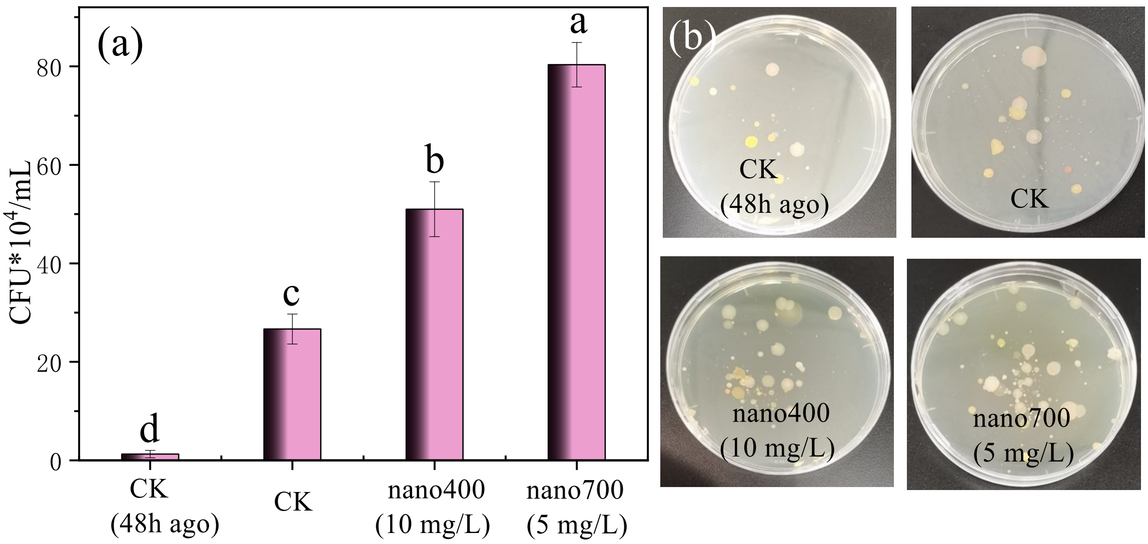

Fig. S9. Results of plate-counting assays for the microorganisms assembled on the iron plaque of rice roots in the presence and absence of nano-BC (nano400 and nano700). The concentrations of microorganisms in the plates (a) and the images of microorganism assemblages for nano-BC treatments and control (b).

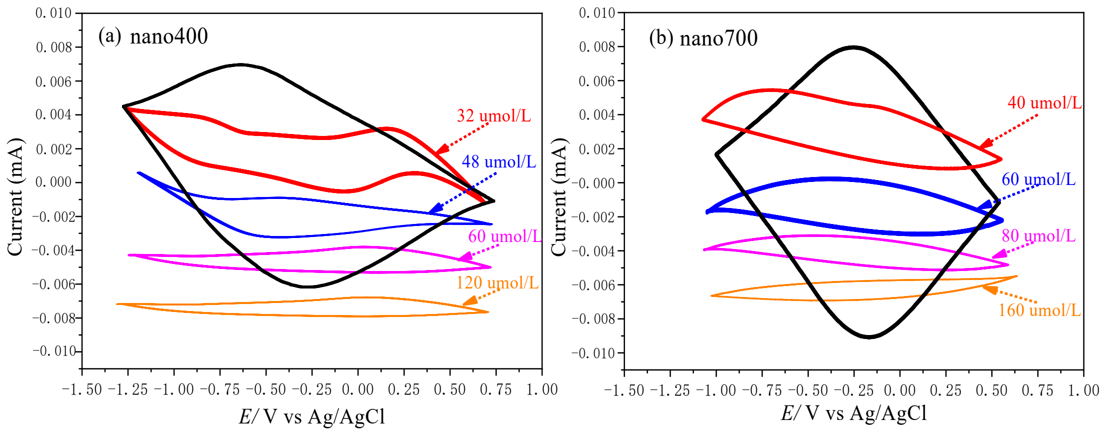

Fig. S10. Voltammetric analyses of nano-BCs (nano400 and nano700) treated by different concentrations of tert-butyl alcohol (TBA).

Table S1. The physiochemical properties of nano-BCs

BC	Surface functionalities and atomic content (%)										TOC	S_{BET} [a]	V_{tot} [b]	*D* [c]
	C	O	N	O/C	(N+O)/C	Si	Ca	C-C	C-O	C=O	(mg/L)	(m^2/g)	(cm^3/g)	(nm)
nano700	54.8	31.5	1.6	0.57	0.60	10.8	2.0	47.1	29.4	23.5	28.29	253.9	0.58	220
nano400	55.0	32.4	2.4	0.58	0.63	8.6	1.6	45.8	24.8	29.4	14.89	93.18	0.36	280

[a] S_{BET} is surface area calculated by the Brunauer-Emmett-Teller (BET) method from adsorption isotherms;

[b] V_{tot} is total pore volume measured by nitrogen adsorption−desorption at 77 K using an Autosorb-1 gas analyzer, determined at P/P_0=0.99;

[c] *D* is the hydrodynamic diameter measured by a dynamic light scattering analyzer at room temperature

Table S2. Composition of the artificial rhizosphere solution used for hydroponic culture of rice seedlings

Number	Macronutrients	Concentration (mg/L)
1	$Ca(NO_3)_2*4H_2O$	10
2	KCl	1.2
3	KH_2PO_4	2.5
4	$MgSO_4*7H_2O$	2.5
Number	micronutrients	Concentration (μg/L)
1	KI	0.3
2	LiCl	0.3
3	$CuSO_4*5H_2O$	0.6
4	$ZnSO_4*7H_2O$	1.1
5	H_3BO_3	0.6
6	$Al_2(SO_4)_3$	0.6
7	$MnCl_2*4H_2O$	3.9
8	$NiSO_4*7H_2O$	0.6
9	$Co(NO_3)_2*6H_2O$	0.6
10	KBr	0.3
11	$(NH_4)_6Mo_7O_{24}$	0.6

Table S3. The selected nutrient concentrations in the shoots and roots of rice plants cultured in the aqueous suspension of nano-BC (nano400) *

Nano-BC	Nutrient concentrations (ug/g)									
(mg/L)	N	P	K	Ca	Mg	Mn	S	Cu	Fe	Zn
Nano400	Roots									
0	2889±67.2c	2541±75.9bc	4698±96.3c	2669±50.3b	1671±6.46a	30.82±0.74cd	12984±253b	91.05±25.0a	1119±112bc	29.94±29.6b
5	3235±30.4c	2648±288c	4841±207bc	3143±67.2c	1851±289a	30.03±5.71bcd	14918±138c	125.5±5.10a	1394±176c	35.38±8.94c
10	3971±184d	2888±423c	5313±144d	3743±22.6d	1937±68.9a	36.49±14.0d	18054±126d	144.1±21.8b	2618±110d	39.73±15.2d
20	1951±236b	2542±285bc	4771±150b	3245±341c	1759±231a	27.76±4.89c	15690±163b	115.8±2.62a	1074±138ab	37.71±1.30c
40	1252±43.9a	2074±84.6ab	4454±149ab	2175±118ab	1268±51.2a	22.19±1.02ab	10427±129bc	116.8±12.9a	930.4±127a	21.48±1.78a
80	1167±168a	1757±146a	3606±97.9a	2011±249a	1118±134a	17.73±1.13a	9837±138a	82.9±10.9a	919.2±54.5a	16.00±14.8a
Nano400	Shoots									
0	3115±64.5b	9259±68.6a	50176±515a	8033±687b	6904±420a	795.3±91.5c	4053±38.5a	26.61±0.04b	1142±0.58a	106.6±12.3bc
5	3676±177bc	9794±237ab	51785±154a	8953±281b	7776±271a	829.5±290c	4046±42.4a	28.02±6.98b	1691±261a	113.9±32.4c
10	4106±70.7c	11200±136b	58047±200b	10867±174c	8940±308a	851.0±108c	5057±45.2a	36.46±1.24c	1854±204b	126.1±6.66c
20	2100±19.9a	9994±78.6ab	50629±772a	8789±616ab	6792±360a	591.9±71.0b	4887±518a	27.81±2.30b	1404±183a	89.9±3.41ab
40	2045±316a	8618±104ab	45543±249ab	6850±141a	5983±68.3a	539.8±2.78ab	4417±641a	27.94±0.41b	1448±438a	81.9±8.11a
80	2030±106a	8593±65.3a	42496±630a	6475±102a	5347±105a	440.1±31.1a	3945±19.3a	18.89±8.32a	1482±129a	79.6±10.0a

Different letters represent different statistical groups suggested by the Tukey-HSD multiple comparisons at $P < 0.05$

Table S4. The selected nutrient concentrations in the shoots and roots of rice plants cultured in the aqueous suspension of nano-BC (nano700) *

Nano-BC	Nutrient concentrations (ug/g)									
(mg/L)	N	P	K	Ca	Mg	Mn	S	Cu	Fe	Zn
Nano700					Roots					
0	2889±67.0b	2541±76.0bc	4698±96.3ab	2669±50.3a	1671±6.46a	30.82±0.74ab	12984±253a	94.05±25.0ab	1119±112a	29.94±29.6ab
5	3400±305c	2736±1.69b	6967±230b	3545±236bc	2317±129.9ab	60.15±16.3c	10482±564a	94.95±14.1ab	2077±67.3b	46.34±0.96c
10	2755±140b	2263±355abc	5734±156ab	3395±610ab	2425±150ab	26.39±1.26a	12561±186a	113.0±3.37b	1458±85.1a	37.74±4.53b
20	1960±40.5a	1954±328ab	3366±260a	4260±287c	2541±351b	38.26±2.50b	14453±201a	94.59±8.67ab	1260±150a	28.09±25.5ab
40	1689±353a	1864±319a	4102±328ab	3558±179bc	2411±91.0ab	38.83±5.82b	13650±243a	93.94±18.0ab	1203±276a	24.84±9.65a
80	1460±427a	1844±199a	2994±399a	3445±338bc	2249±289ab	37.73±0.19b	13936±164a	79.95±4.55a	1164±112a	27.81±27.2ab
Nano700					Shoots					
0	3115±64.5b	9259±68.6b	50176±515b	8033±687b	6904±419b	795.3±91.5b	4553±38.5a	26.61±0.04a	1142±0.58b	106.6±12.3bc
5	4005±179c	13086±296c	91811±475c	15035±636d	8340±446c	1013±414c	6626±97.3a	38.10±4.78c	1740±93.4c	116.6±40.8c
10	3191±35. 9b	11030±895b	58922±138bc	10840±378c	7213±79.3bc	759.1±52.7b	5127±38.0a	30.52±2.31b	1673±185c	103.6±1.65bc
20	2017±7.66a	8379±615b	65589±143bc	10927±275bc	6424±165a	812.1±355b	5544±302a	27.14±3.78ab	1008±15.8ab	92.31±17.1ab
40	2023±92.1a	6611±97.0a	41157±106a	6003±62.2a	5648±33.5a	334.0±1.68a	3856±705a	30.56±4.85b	940±81.7a	86.97±2.64a
80	1821±64.0a	5641±88.8a	41628±264a	5961±149a	5664±243c	303.2±12.2a	4126±158a	27.09±9.44ab	912±158ab	72.76±10.5a

* Different letters represent different statistical groups suggested by the Tukey-HSD multiple comparisons at $P < 0.0$